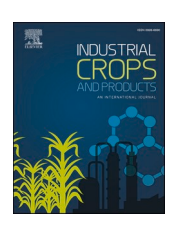
ELSEVIER

Contents lists available at ScienceDirect

Industrial Crops & Products

journal homepage: www.elsevier.com/locate/indcrop





Energy-efficient and improved productivity of cellulose nanofibril processing in wet disc mill by regulating the cellulose degree of polymerization

Liana Noor Megashah ^a, Hidayah Ariffin ^{a,b,*}, Mohd Rafein Zakaria ^a, Yoshito Andou ^c, Mohd Ali Hassan ^a, Tengku Arisyah Tengku Yasim-Anuar ^a

- a Department of Bioprocess Technology, Faculty of Biotechnology and Biomolecular Sciences, Universiti Putra Malaysia, Serdang, Selangor 43400 UPM, Malaysia
- b Laboratory of Biopolymer and Derivatives, Institute of Tropical Forestry and Forest Products (INTROP), Universiti Putra Malaysia, Serdang, Selangor 43400 UPM, Malaysia
- ^c Kyushu Institute of Technology, 2-4 Hibikino, Wakamatsu-ku, Kitakyushu, Fukuoka 808-0196, Japan

ARTICLE INFO

Keywords: Cellulose nanofibril Oil palm biomass Energy efficient Productivity Energy-neutral pretreatment Lab-scale nanofibrillation

ABSTRACT

This research highlights the use of superheated steam (SHS) treatment to improve the productivity and reduce the energy consumption of CNF processing. SHS treatment conducted at 150° C for 1 and 2 h (SHS1 and SHS2) contributed to the reduction in degree of polymerization (DP) of cellulose from oil palm empty fruit bunch. Results exhibited that SHS-treatment reduced the viscosity and number of cycles for CNF processing compared to the untreated cellulose (UT). At the end of wet disc mill processing, CNF-SHS2 viscosity was measured at 60 cP, almost five-fold lesser than that of CNF-UT. The productivity of CNF-SHS2 production improved by almost eightfold compared to CNF-UT, and the energy consumed to produce CNFSHS2 reduced from 60.5 to 7.4 kWh/kg. All CNF samples produced had an average width of about 10 nm and crystallinity between $54-62^{\circ}$ %. Our results showed that treatment of cellulose by SHS prior to nanofibrillation contributed to energy efficient nanofibrillation process with improved productivity. The potential energy neutral SHS treatment is demonstrated herein by integrating the energy resource available at the palm oil industry towards sustainable CNF production which would promote the commercial potential of this versatile bio-based material.

1. Introduction

Cellulosic biomass from agricultural residues can be converted into versatile nanomaterials applicable to various industries. The development of cellulose nanofibril (CNF) from cellulosic biomass such as sweet sorghum bagasse, sugar palm fibers, oil palm fibers, arecanut husk fibers, raw cotton linter, bamboo, etc. has been reported earlier (Ganesh Kumar et al., 2015; Ilyas et al., 2018; Julie Chandra et al., 2016; Megashah et al., 2018a; Morais et al., 2013; Ramírez et al., 2019). CNFs are long, flexible, and entangled nanoscale fibrils (Hietala et al., 2018). The unique properties of the material such as high surface area, high hydrophilicity, high mechanical properties, and has a gel-like appearance have made the CNFs to receive attention from the industries for various applications (Klemm et al., 2011). Among the applications are as a filler in polymer-based composites (Ariffin et al., 2018; Siró and Plackett,

2010), an additive in the papermaking process (Bardet and Bras, 2014) and as a low-calorie thickener for pharmaceutical/foods products (Klemm et al., 2011; Spence et al., 2011). CNF also has been used as the primary material for the production of optical transparent film and coating materials (Huang and Wang, 2017; Hwangbo et al., 2016; Megashah et al., 2020).

There have been several commercial plants for producing CNF. Nevertheless, the widespread application of CNF is still limited, mainly due to the manufacturing readiness level. The high energy demand for the production of CNFs which leads to the high cost of this nanomaterial has been the major hindrance in its commercial application. Conventionally, CNFs are produced by mechanical approaches such as high-pressure homogenization (Sánchez et al., 2016; Yang et al., 2017), ultrasonication (Yasim-Anuar et al., 2018; Zhao et al., 2015), cryo-crushing (Alemdar and Sain, 2008), microfluidization (Wang et al.,

E-mail address: hidayah@upm.edu.my (H. Ariffin).

^{*} Corresponding author at: Department of Bioprocess Technology, Faculty of Biotechnology and Biomolecular Sciences, Universiti Putra Malaysia, Serdang, Selangor 43400 UPM, Malaysia.

2015a; Wang et al., 2015b), and refining/ grinding (Chang et al., 2012; Qin et al., 2016). Homogenization and refining are the most common methods used for CNF production (Siró and Plackett, 2010). Despite their efficiency in disintegrating the cellulose into CNFs, several issues have been associated with these methods. For instance, the main issue with homogenization is the extensive clogging when the cellulose pulp is pumped through the narrow nozzle at the moving part of the machine. This slows the production as frequent cleaning is needed. High number of passes also contributes to the high energy demand, commonly in the range of 20–70 kWh/kg (Boufi and Gandini, 2015; Spence et al., 2011).

In the case of refining, the most common method is the wet grinding method using a wet disc mill (WDM), or commonly reported as Masuko Supermasscolloider grinder (Levanič et al., 2020; Rambabu et al., 2016; Rol et al., 2017; Wang and Zhu, 2016). The process involves the use of frictional force by placing the cellulose suspension between the static and rotating grinding stones at rotational speed of 1500-1800 rpm (Abe et al., 2007; Iwamoto et al., 2008; Teixeira et al., 2015). This method is capable of producing CNF suspension with solid content ranging from 1 - 3 wt% (Eriksen et al., (2008); Iwamoto and Endo (2015). Other notable advantages of WDM compared to homogenization is that the process is capable in defibrillating fibers at a higher consistency and having a faster processing time, thus, making it easier for large-scale CNF processing (Hietala et al., 2018; Wang and Zhu, 2016). Nevertheless, similar to other mechanical methods, the major obstacle of WDM is that it requires high energy demand between 5 - 30 kWh/kg (Berglund et al., 2016; Josset et al., 2014; Spence et al., 2011). High energy consumption can be a significant challenge in the industrial production of CNF and is a concern for sustainability and cost-effectiveness (Balea et al., 2021).

One of the factors that contributes to the high energy processing of CNF is the cellulose fibril length. Longer cellulose fibrils were found to increase the fibrillation time to disintegrate micro to nanofibrils (Wang and Zhu, 2016). As a consequence, energy consumed will be higher. Pretreatments such as acid and enzymatic hydrolysis have been introduced to reduce the energy demand during CNF fibrillation process (Balea et al., 2021; Hubbell and Ragauskas, 2010; Liu et al., 2018; Qin et al., 2016; Wang et al., 2015; Zhu et., 2011). The pretreatments reduce fiber entanglement, which helps prevent blockages during mechanical fibrillation. In our previous work (Megashah et al., 2020), we reported the use of superheated steam (SHS) as a superior method for cellulose depolymerization, and the resultant CNFs were used to prepare nanofilm. The CNF films produced had versatile characteristics due to the difference in the degree of polymerization (DP) after the SHS treatment. SHS treatment resulted in increased stiffness of the CNF films, as evidenced by higher Young's modulus values based on previous study (Megashah et al., 2020). This indicates that despite any potential reduction in the degree of polymerization, the SHS treatment enhances the mechanical properties of CNF.

SHS is a dry, saturated steam that has been heated to a temperature above its boiling point at a specific pressure (Alim et al., 2022; Challabi et al., 2019; Rajaratanam et al., 2017), making it a thermodynamically stable state with no liquid water present. Unlike steam explosion which uses high-pressure steam to break down the lignocellulosic structure for bioethanol production (Barchyn and Cenkowski, 2014), SHS is primarily used for hydrolysis, breaking the glycosidic bonds that link glucose units in the cellulose polymer chain resulting in the cleavage of cellulose molecules into smaller fragments to reduce its DP. SHS treatment also loosens the structure of cellulose fibers and causes cellulose swelling, making them more accessible to mechanical processes which is beneficial for applications like CNF production from WDM. Reducing the DP of cellulose enhances the flow properties of CNF suspension, lowering viscosity and fibrillation time, thus improving energy efficiency and overall productivity in CNF processing. Despite the lack of prior studies on SHS for cellulose pretreatment for CNF production, this study focused on investigating its potential in manipulating cellulose DP by SHS and its effect on the flow property (viscosity), energy consumption and productivity of the CNF processing, particularly using oil palm empty fruit bunch (OPEFB). This study also evaluated the economic feasibility of this sustainable approach for industrial applications.

2. Experimental

2.1. Materials

Bleached pulp was prepared from oil palm empty fruit bunch (OPEFB) fibers as reported in previous works (Megashah et al., 2018a; Megashah et al., 2018b). The cellulose purity of the bleached pulp was determined to be 93 % with the remaining of 7 % comprising hemicellulose. Pulping was conducted in a 15 L batch reactor of a lab-scale twin digester (model GTD-15L, GIST Co Ltd., Korea). OPEFB fibers were mixed with 14 % alkali charge of sodium hydroxide solution at a ratio of 1:4 and cooked for 1 h at 160°C with a pressure of about 0.5 MPa. The treated cellulose pulp was then washed several times using tap water until the pH became neutral. For bleaching, a Totally Chlorine Free (TCF) treatment was introduced. Dried pulp was soaked and stirred in a peracetic acid solution for 24 h at 70°C. The cellulose samples obtained were then washed and subsequently dried at 60°C overnight.

2.2. Depolymerization of OPEFB cellulose pulp by superheated steam (SHS) treatment

SHS treatment was conducted in a lab-scale superheated steam oven (QF-5200C, Naomoto Corporation, Osaka, Japan) at ambient pressure. The SHS treatment temperature was maintained at 150°C throughout the whole experiment. SHS treatment was conducted for 1 h (SHS1) and 2 h (SHS2). At these conditions, cellulose was depolymerized into lower DP cellulose without involving the weight loss (except due to moisture removal). Lower DP cellulose can be obtained if the treatment time is prolonged, however this will reduce the mechanical properties of the cellulose. It was hence the SHS treatment was limited to 2 h. The DP of untreated cellulose pulp (UT), and SHS-treated cellulose pulp (SHS1 and SHS2) was measured as mentioned in the previous report (Megashah et al., 2020). Cellulose DP was determined by determining the intrinsic viscosity of cellulose solution using the viscometric technique according to the standard test method, TAPPI T230, ISO 5351 (Henriksson et al., 2008; Marx-Figini, 1978). The DP of the cellulose pulp is summarized in Table 1.

2.3. Preparation of cellulose nanofibrils by wet disc mill

CNF was produced by WDM (Multi mill, Grow Engineering, Adachiku, Tokyo, Japan). In a WDM setup, there are two millstones: one upper and one lower. The upper millstone remains stationary, meanwhile, the lower millstone rotates during operation. This study employs a two-stage grinding approach, utilizing varied types of stones for each stage. The initial stage employs coarse stones (Type VC15–46A), followed by the subsequent stage using smooth stones (Type $\alpha VCi15–46$). Initially, the untreated and treated cellulose pulps were soaked in distilled water for 72 h at a known quantity, whereby the cellulose

Table 1

The degree of polymerization and molecular weight of cellulose pulp from different conditions of SHS treatment.

Cellulose samples	Degree of polymerization ^a	Molecular weight, gmol ^{-1 b}
UT	1440 ± 28.5	$222,\!000 \pm 2.9 \times \! 10^3$
SHS1	1030 ± 25.5	$171,\!000 \pm 4.1 \times \! 10^3$
SHS2	820 ± 10.5	$133,\!000 \pm 4.0 \times \! 10^3$

Notes:

 $[^]a$ DP determination was calculated from the intrinsic viscosity, $\eta,$ using $[\eta]=0.42DP$ for DP <950 and $[\eta]=2.28DP$ $^{0.76}$ for DP >950.

 $^{^{\}rm b}$ MW = DP x (162 g/mol), whereby 162 g/mol is the molecular weight of an anhydroglucose unit.

content was set to be in the range of 1-4 wt% prior to milling. The cellulose suspension was then subjected to the grinder, in which coarse stones were used for the first 10 cycles to initiate early fibrillation, followed by another 10 cycles using smooth stones to ensure the formation of nano-scale size of CNFs. The distance between the upper and lower stones was adjusted to be less than 50 micrometers from initial contact and the rotational speed was set at 1800 rpm (Iwamoto and Endo, 2015; Megashah et al., 2018a; Yasim-Anuar et al., 2020). Fig. 1 shows the overview of CNF processing in this study.

2.4. Energy consumption

Energy consumed during the CNF fibrillation by WDM was evaluated using a portable power meter (UNI-T UT200, 1000 A Series, China) to measure the current flow (amps) and the voltage (volt) (Malucelli et al., 2019). The calculation was based on the alternating-current three-phase plug by the line to neutral voltage. For the induction load applied to the rotating milling stones, the power factor was approximately 0.85 and the voltage equals to 450 volts. The power consumption is in the unit of kW and the specific energy is in kWh per kg of samples. The formula for power and energy is as shown in the Eq. (1):

$$Power(kW) = \frac{3 \times PF \times amperes (I) \times volts (line to neutral)}{1000}$$
 (1)

Where, PF = power factor, I= current (amps) and voltages (volts) are generally subjected to the three-phase system, in line to neutral. The value of power consumption will be used for calculating the specific energy as in Eq. (2). Where, mass throughput expressed in h/kg of grinding time is the total hours of complete cycles for per kg of cellulose pulp.

$$Specific \ energy \left(\frac{kWh}{kg} \right) = Power(kW) \quad \times mass \ throughput \left(\frac{h}{kg} \right) \quad \ (2)$$

The reduction in energy consumption was calculated based on the baseline energy consumption (E₀) at 20 cycles and ΔE is the absolute reduction in energy consumption.

Percentage Reduction(%) =
$$\left(\frac{\Delta E}{Eo}\right) x 100\%$$
 (3)

2.5. Characterization

2.5.1. Field emission - scanning electron microscopy (FE-SEM)

The morphology of the CNFs were observed using a field emission scanning electron microscope (FE-SEM; JEOL 7500 Ltd., Japan). The CNF was freeze-dried prior to FE-SEM analysis. The samples were then coated with Pt using Hitachi Ion Sputter E-1030 and the images were

viewed at 100,000 x magnification with 15 kV of beam voltage.

2.5.2. High resolution - transmission electron microscopy (HR-TEM)

Further morphological analysis was conducted using high resolution - transmission electron microscopy (HR-TEM; JEOL Ltd.) to confirm the diameter size of the nanofibril. The CNF suspensions were diluted to 0.1 % (v/v) and sonicated using Thermo-6D ultrasonic cleaner for 15 min to ensure homogeneous dispersion of the CNF in the suspension. The ultrathin carbon film on copper grids was placed on a drop of CNF solution with uranyl acetate and allowed to stain for 5 min. This dispersing agent helps in breaking the CNF bundles and keeps in individual fibrils (Foster et al., 2018). Then, the prepared sample was viewed under HR-TEM. The J-Images analysis software was used to measure the diameter and distribution of the viewed CNF where the fibers were randomly selected for size distribution analysis, with a consistent total of 30 measurements conducted for each sample. The method involved measuring the diameter size of CNF in the horizontal direction of each fiber. The counts in a bin were presented in histogram data.

2.5.3. Crystallinity

The crystallinity index (CrI) of cellulose and CNFs was determined using a benchtop X-ray Diffractometer (XRD) model Rigaku MiniFlex. The operating condition was set at 40 kV and 15 mA. The data was collected at 20 value between 5 and 50° with a scan speed at 2.0°/min. The CrI was calculated based on Segal's method (Eq. 3) (Segal et al., 1959), whereby I_{200} is the intensity of the highest peak (I_{200}) at 20 around 22.5°, while I_{am} is the minimum intensity of the amorphous region at 20 around 18.5°. The intensities were in agreement to the observed pattern in Segal's peak height (Ling et al., 2019).

$$CrI(\%) = \frac{I_{200} - I_{am}}{I_{200}} \times 100\%$$
 (4)

2.5.4. Thermogravimetric analysis

The thermal stability of samples was analyzed using a thermogravimetry analyzer (TG 400, Perkin Elmer, Waltham, MA, USA). TG analysis was conducted at a temperature range between 50° C to 550° C with a heating rate of 10° C/min. Nitrogen was purged at a flow rate of 100 ml/min.

2.5.5. Rheological properties

The rheology of different CNF suspensions was determined using a rheometer instrument (DV2T, Brookfield, USA). The analysis was conducted at ambient temperature and LV-04 (64) type spindle was used. The rotational viscometer was performed in continuous measurement of the friction torques. The reading of viscosity was recorded in a unit of centipoise (cP). Each sample was run five times.

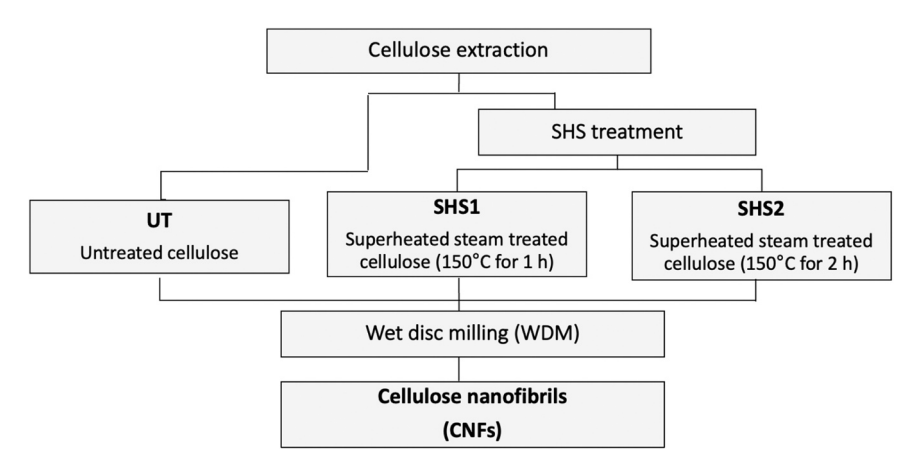


Fig. 1. Overview of the CNF production by wet disc milling.

2.6. Economic assessment of cellulose nanofibrils processing

The economic assessment was determined at two process phases: pretreatment for cellulose isolation and the process of nanofibrillation. In comparison, the SHS treatment process model was compared to without pretreatment for CNF production. Three key parameters were taken into account including capital expenditure (CAPEX), operational expenditure (OPEX) and profitability analysis. The calculations were performed by referring to engineering economic multiplier values (Peters et al., 2003). The assessment was based on the technical data projected for 1-tonne CNF production using the data of production rate and product yield obtained.

3. Results and discussion

3.1. Determination of the suitable number of cycle for complete nanofibrillation of cellulose in wet disc mill

A preliminary evaluation was performed to determine the WDM number of passes for CNF production. In this study, untreated cellulose was used. Fig. 2., shows the morphological effect of the number of passes (5, 10, 15, 20 and 30 cycles) on the morphological properties of the cellulose. The diameter of the samples were quantified and shown in Table 2. It is worth noted that the dimension of the original cellulose fiber was more than 0.2 µm which was in micro size. After 5 passes, thinner fibril bundles were partially disintegrated with a minimum diameter of about 100 nm. It was observed that the fibrils network started to create single nanofibrils after 15 cycles of milling. However, there was still a large number of fibrils having a diameter of more than 100 nm, indicating that the cellulose did not disintegrate homogeneously. Continuous milling up to 20 and 30 cycles created smaller nanofibrils aggregates which then resulted in homogenous disintegration into single nanofibrils with less than 20 nm. Subsequent cycles up to 30 did not show any noticeable changes, yet may cause a detrimental effect on the fibrils such as low crystallinity and strength properties (Rojas et al., 2015). Based on this result, 20 cycles was set as the suitable number of passes for the next experiment, which was to compare the effect of degree of polymerization on the formation of CNF.

Table 2Effect of number of cycles (WDM) on the diameter size of fibrillated UT cellulose.

	Cycle 0	Cycle 5	Cycle 10	Cycle 15	Cycle 20	Cycle 30
Average diameter (nm)	226.37	106.40	75.30	56.17	18.18	11.81
SD	58.21	20.08	17.65	12.13	10.84	2.66
Min	147.58	90.28	48.41	11.58	9.81	8.31
Max	309.74	120.50	108.80	108.16	53.29	19.18

Notes: SD = Standard deviation, Min - observation of lowest diameter size range, Max - observation of highest diameter size range

3.2. Effect of degree of polymerization on dispersion behavior and morphology of cellulose nanofibrils

Fig. 3 demonstrates the effect of DP on the evolution of fiber dispersion in cellulose suspension during wet disc milling. The color change observed in cellulose after SHS treatment can vary depending on the treatment condition. Cellulose can undergo thermal degradation and may appear yellowish. In this work, SHS treatment involves exposing cellulose to high temperatures and the reason why SHS2 with longer exposure to temperature is more likely to result in a darker color. These degradation products can be the result of cellulose chain scission. Based on the literature (Shahabi-Ghahfarrokhi et al., 2015; Thi et al., 2015), the dispersion state can be used to qualitatively determine the degree of fibrillation. The samples were collected at every two cycles and stored at room temperature for more than three months to observe the stability of CNFs to be freely dispersed in water. From the observation, it was demonstrated that SHS1 and SHS2 caused the cellulose to be easier dispersed in water compared to UT. This can be seen from the absence of phase separation started at 14th and 8th cycle for SHS1 and SHS2, respectively, compared to UT which achieved complete dispersion at 18th cycle. Complete dispersion contributed to increased viscosity. According to Henriksson and Berglund (2007), the viscosity of the cellulose fiber suspension increases during CNF preparation due to the increase in the length-to-diameter ratio of the fiber. As a result, reduced DP accelerates the rise in viscosity, as a reliable indicator of the degree of nanofibrillation within the suspension. Findings from this research

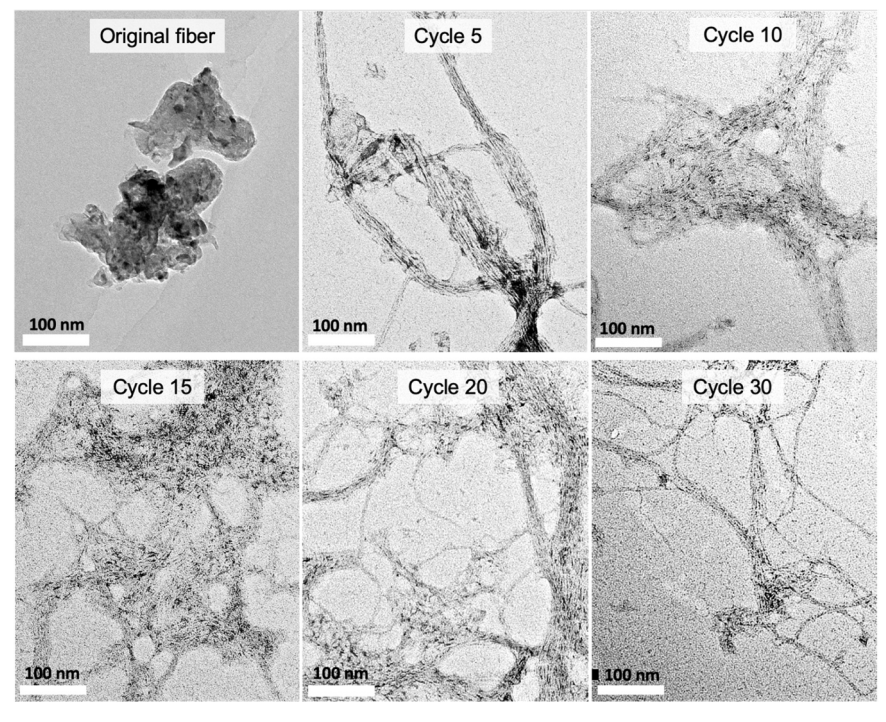


Fig. 2. TEM micrographs of fibrillated UT cellulose (1 wt%) after 0, 5, 10, 15, 20 and 30 milling cycle.

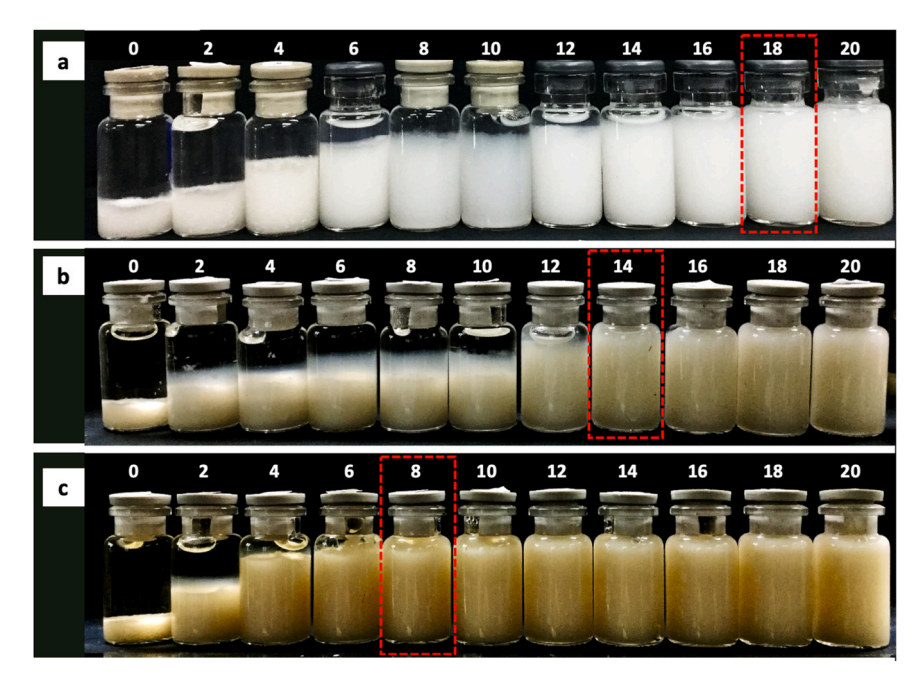


Fig. 3. Visual appearance of dispersion state of fibrillated cellulose at a concentration of 1 wt% for sample; (a) UT; (b) SHS1 and; (c) SHS2. L-R: 0th cycle (at the start of experiment) – 20th cycle (at the end of the experiment). Red dashed lines indicate the number of cycle at which complete fibrillation (no phase separation) started to be observed.

indicated that lower DP of cellulose improved the degree of nanofibrillation. Cellulose with a lower DP contributes to easier mechanical disintegration due to the shorter chain and more susceptible to mechanical forces, making them easier to break apart. The DP can have a pronounced effect on the dissolution behavior of cellulose, where previous studies reported that cellulose with a lower DP tends to exhibit higher swelling, while cellulose with DP less than 500 is somewhat dissolved and led to a molecular-disperse solution with no visible structure when observed under the optical microscope (Koistinen et al., 2023). However, swelling behavior can be influenced by temperature and pressure. Thus, it is important to control the temperature and treatment duration during SHS treatment in response to changes in DP.

This study revealed that increasing the number of milling cycles resulted in the increment in its surface area. In agreement with Fig. 2,

vigorous mechanical fibrillation through WDM typically disrupts the cell wall of cellulose and promotes the higher separation of aggregated fibrils. It also contributes to thinner cellulose fibrils by the formation of hydrogen bonds around the fibrils and thus, exposing the hydroxyl groups of cellulose chains to conformationally ordered (Boufi and Gandini, 2015; Tayeb et al., 2018). This phenomenon is also known as the electrostatic dipole-dipole of cellulose-water interaction where the water with a negative charge tends to bind with cellulose chains with a positive charge and vice-versa (Khazraji and Robert, 2013). In this case, the SHS2 sample has much lower cycles which only required coarse stones to complete the nanofibrillation process. This attributed to one grinding process for CNF production. It is envisioned that the actual cycles can be further used to produce CNF and the diameter sized were further analyzed.

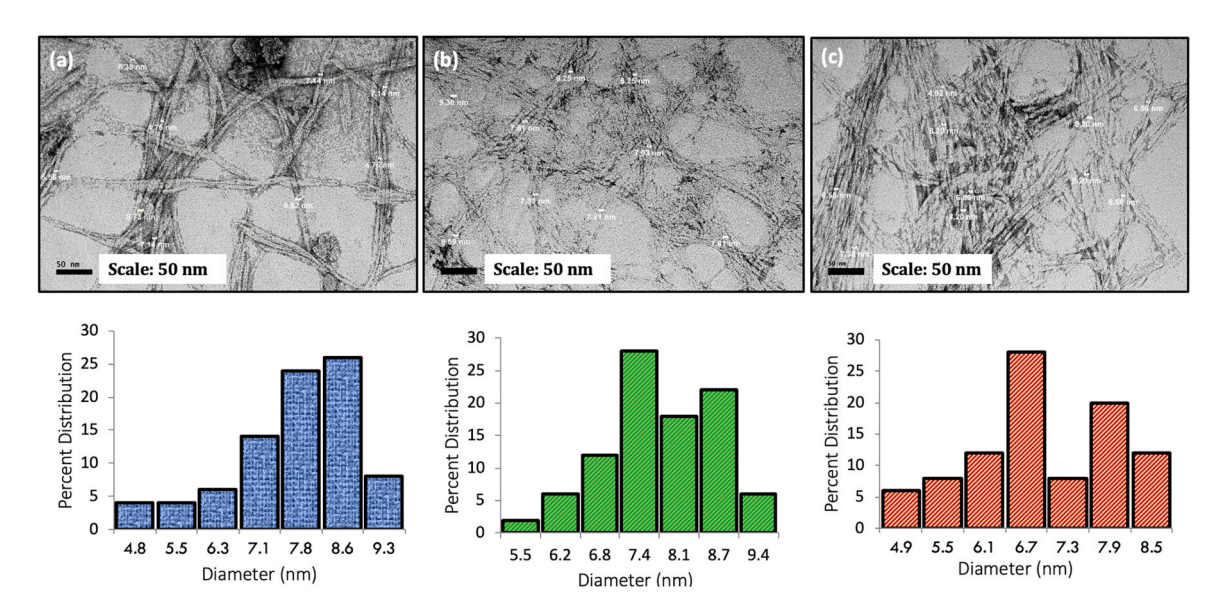


Fig. 4. The diameter size distribution of single nanofibril at cycle 20 through WDM processing, (a) CNF-UT; (b) CNF-SHS1; and (c) CNF-SHS2. Note: The elevated bin represents the higher distribution size of nanofibrils from CNF suspension, while the lowest recorded the minimal distribution.

Next, the diameter size of the fibrillated samples was obtained through the analysis of FE-SEM and HR-TEM. From the results, the diameter of CNFs at different DPs were below 50 nm. Despite the difficulties to obtain individual nanofibrils from FE-SEM images, the wellindividualized nanofibrils could be observed using TEM. Fig. 4 displays the diameter of the CNFs from TEM images at a scale bar of 50 nm which represents the final cycles (cycle 20) of each CNF sample and showcases the diameter size distribution in the histogram. The images demonstrated the individualized nanofibril for CNF-UT, CNF-SHS1 and CNF-SHS2 with small aggregation at cycle 20. The result revealed that all individual CNF have comparable diameter, capable of achieving diameter with less than 10 nm despite having different DPs. However, from the images, the highest degree of distribution of the nanofibrils with smaller diameter can be seen from CNF-SHS2, followed by CNF-SHS1 and CNF-UT. For example, CNF-SHS2 has the lowest diameter of nanofibril in approximately 6.7 nm with higher percentage distribution in about 28 %. Whereas, the histogram also shows that the CNF-SHS1 and CNF-UT recorded 13 % and 6 % of nanofibril with a diameter of 6.3-6.8 nm, respectively. The factor contributing to such differences in diameter size of nanofibril may be arising from the heterogeneity of the sample, where the lowest DP is expected to have less fibril network entanglement and thus, dispersed well in CNF suspension (Megashah et al., 2020).

3.3. Effect of number of cycles on the morphological property of different degree of polymerization cellulose nanofibrils

It was exhibited in Fig. 3 that complete nanofibrillation can be achieved at WDM cycle less than 20 for SHS1, SHS2 and UT samples. In order to evaluate the effect of WDM number of cycles on the morphological property of the CNF, an observation was conducted by TEM for the CNF samples produced at cycles 18, 14, and 8 for CNF-UT, CNF-SHS1 and CNF-SHS2, respectively. The findings are shown in Fig. 5. Based on the results, it was observed that the average CNF diameter was slightly larger in the range of 5 – 30 nm, compared to those prepared at 20 cycle WDM (around 10 nm). It is interesting to note that lower DP CNF produced from SHS treated samples resulted in highest distribution with the smallest nanofibrils diameter compared to CNF-UT. Based on the image, a high degree of parallel alignment may suggest lower entanglement,

while a more random and intertwined arrangement could indicate greater entanglement. Nevertheless, it was revealed that the degree of entanglement of nanofibrils is low for all CNF samples, thus, indicated that the actual number of cycle was able to greatly reduced the diameter size and gave CNF with higher disintegration.

3.4. Energy consumption during cellulose nanofibril production in wet disc mill

The energy consumption of nanofibrillation in WDM were compared as shown in Fig. 6. Standard CNF nanofibrillation in WDM is conducted for 20 cycles, while in this study the actual number of cycles for nanofibrillation to occur were recorded at 18, 14 and 8 cycles for CNF-UT, CNF-SHS1 and CNF-SHS2, respectively. This deviation highlights the efficiency of the SHS treatment in facilitating fibrillation within fewer cycles. Furthermore, TEM images provide additional support for the attainment of nanosized fibrils in these samples. The actual number of cycles is used in the calculation of energy consumption instead of the standard number of cycles as the energy consumed can be reduced by shortening the milling cycles. As demonstrated in Fig. 6, the energy input was lower by 13 - 78 % for all CNF produced at an actual number of cycles, as compared to the CNF produced at 20 cycles. Additionally, energy consumption was found to be reduced substantially with DP reduction and subsequently improved productivity as shown in Table 3. For SHS-treated samples, the energy can be reduced from 60.5 kWh/kg (CNF-UT) to 18.2 kWh/kg and 7.4 kWh/kg, respectively for SHS1 and SHS2. The energy input was lower for CNF-SHS2 with about 88 % reduction. It was also observed that the reduction in DP was correlated with the reduction in the viscosity of CNF suspensions. The viscosity was found to be at a minimum for CNF-SHS2 (60 cP), followed by CNF-SHS1 (226 cP), and CNF-UT (347 cP). This result can be explained through the mechanism of SHS which contributed to the scission of the fiber chain, contributing to the less entanglement of the nanofibrils (Megashah et al., 2020) and hence lower viscosity. Lower viscosity eventually improved the processing time for nanofibrillation and contributed to lower energy consumption.

Data in Table 3 also revealed that the crystallinity index was increased by reducing the DP, which was from 55.5 % to 60.3 % after SHS treatment for 1 and 2 h, respectively. Fig. 7(a) is the pictorial view

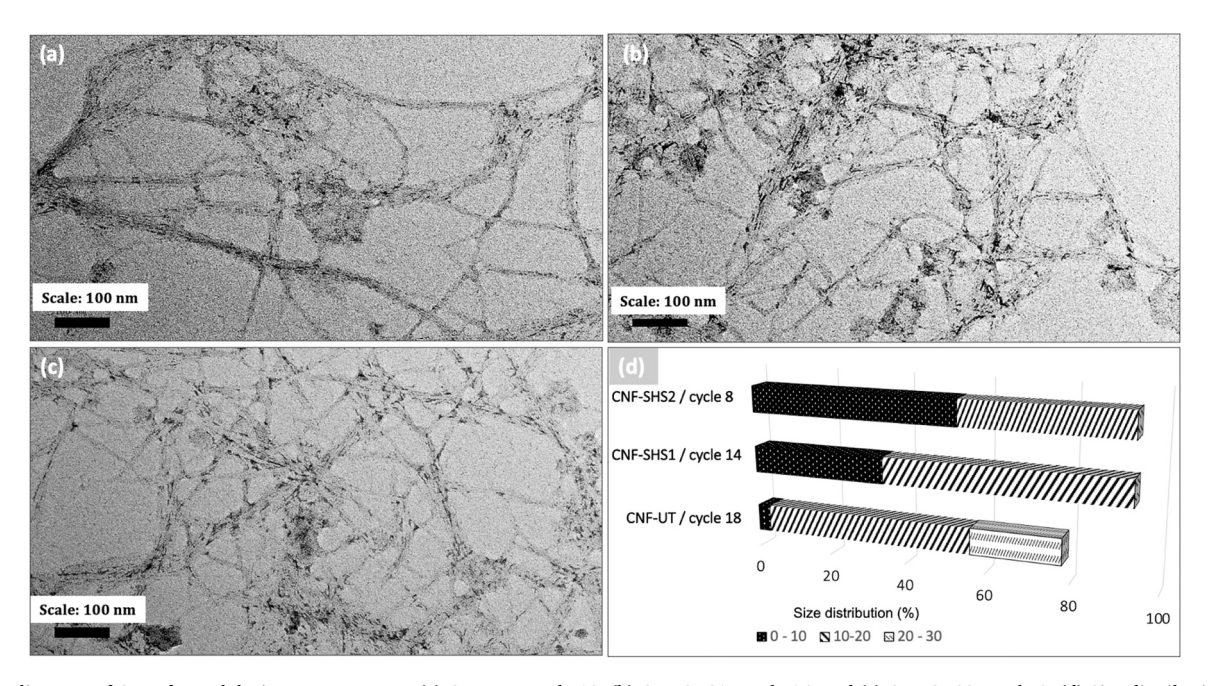


Fig. 5. The diameter of CNFs formed during WDM process. (a) CNF-UT/ cycle 18; (b) CNF-SHS1/ cycle 14; and (c) CNF-SHS2/ cycle 8; (d) Size distribution of three different samples. SHS treatment produced nano-sized fibrils at lower number of WDM cycles.

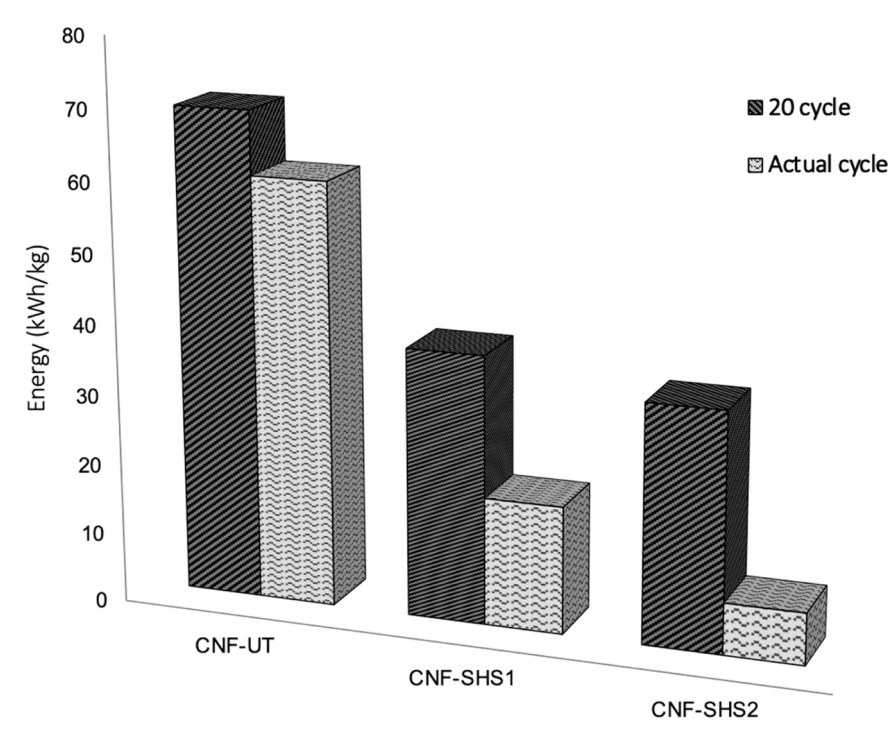


Fig. 6. Energy consumption of CNF samples at 20 cycle and actual cycle from WDM.

Table 3Summary of energy, productivity and properties of CNF samples at actual cycles.

Samples	Energy (kWh/kg)	Productivity (kg/h)	Viscosity (cP)	CrI (%)	T _{max} (°C)
UT/ cycle 18	60.5	0.019	347	55.5	337
SHS1/ cycle 14	18.2	0.060	226	58.2	337
SHS2/ cycle 8	7.4	0.150	60	60.3	341

Notes:

- CrI specifically referring to the Segal method for crystallinity index
- \bullet T_{max} refers to the temperature at which the maximum rate of thermal decomposition occurs during a heating process

of the x-ray diffractograms of the CNFs. In this case, SHS treatment did not only reduce the DP, but also led to the removal of amorphous fibrils. In other words, the SHS treatment selectively removed the noncrystalline regions of the cellulose, leading to an overall increase in the crystallinity of the CNFs. Meanwhile, the TGA curves (Fig. 7(b)) exhibited that there were no significant variations in term of thermal stability for all CNF samples. This indicates that the reduction in DP did not adversely affect the thermal stability of the CNFs.

3.5. High cellulose throughput processing for cellulose nanofibrils production

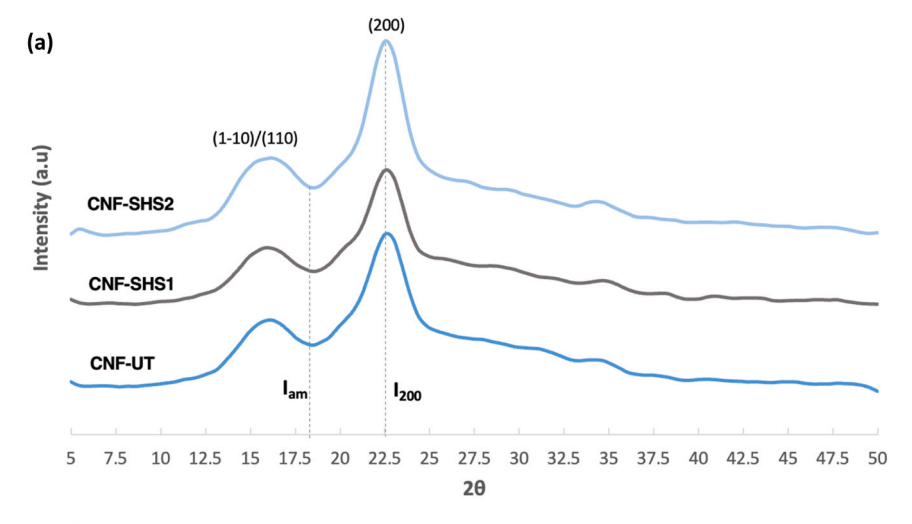
It was postulated that lower cellulose DP may allow for a higher cellulose throughput processing due to the reduction in viscosity. Fig. 8 shows that the energy consumption was in the range of 4.2–42.3 kWh/kg for CNF-SHS2, CNF-SHS1 and CNF-UT processed with solid content of 4 wt%. This is lower compared to the CNF processed at a solid content of 1 wt% (Table 3). The productivity on the other hand was within the higher range (0.044–0.320 kg/h) for CNF processing using 4 wt% solid content, compared to 0.019–0.150 kg/h for the processing at 1 wt% solid content. This finding shows that the solid content during CNF processing affected the energy consumption and productivity, in which

the higher throughput processing contributed to lower energy consumption and higher productivity processing.

The reduction in DP has made higher throughput processing even more advantageous, with a decrement by 10 times in energy consumption, and an increment by more than 7 times in productivity. This observation is related to the viscosity of the CNF suspension (Table 4). The viscosity was reduced from 13,200 to 2580 cP when the DP was reduced from 1440 (CNF-UT) to 820 (CNF-SHS2). As mentioned earlier, DP reduction reduced fiber entanglement and hence reduced viscosity and easier processing.

3.6. Technical evaluation of the high throughput CNF processing using WDM

In order to the evaluate technical feasibility of the high throughput CNF processing, a comparison was made with other findings in terms of the different pretreatment methods used and the type of fibrillation process, as presented in Table 5. Recent studies have shown that the energy demand of wet grinding or WDM for CNF production is lower compared to those of homogenizer and microfluidizer. It is also important to note that the energy consumption may differ with the literature data when using various sources and pretreatments. For example, Spence et al. (2011) used the same pretreatment (e.g. valley beater) with different nanofibrillation process, which resulted in higher energy demands for homogenizer processing (21.9 kWh/kg) as compared to the wet-grinding process (3.6 kWh/kg), respectively. In the case of homogenizer, the mass throughput is low with the reported concentration of 0.7 wt% cellulose. Higher concentration CNF processing at 2 wt% cellulose has been reported by Boufi and Gandini (2015), and oxidation was used as the pretreatment method. Nevertheless, the energy demand was high at about 40 - 45 kWh/kg. The use of endoglucanase pretreatment on the bleached pulp was evaluated, and it was found that the energy required was around 8.5 - 14.0 kWh/kg (Liu et al., 2018; Nair et al., 2014). In this work, higher productivity was achieved through SHS pretreatment, whereby increased concentration of cellulose up to 4 wt% was able to improve productivity with lower energy consumption. The present study is in agreement with the other reported data whereby it is possible to reduce both the milling time and energy



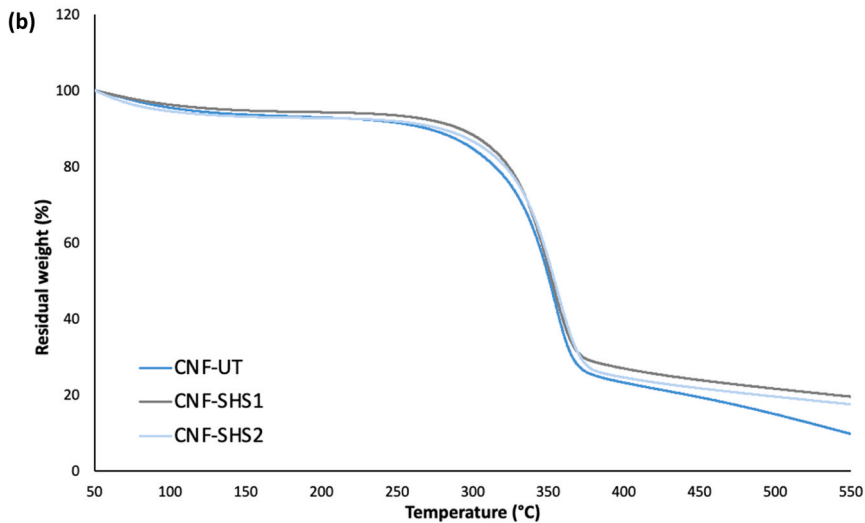


Fig. 7. (a) XRD patterns and (b) TGA curves of CNF-UT, CNF-SHS1 and CNF-SHS2.

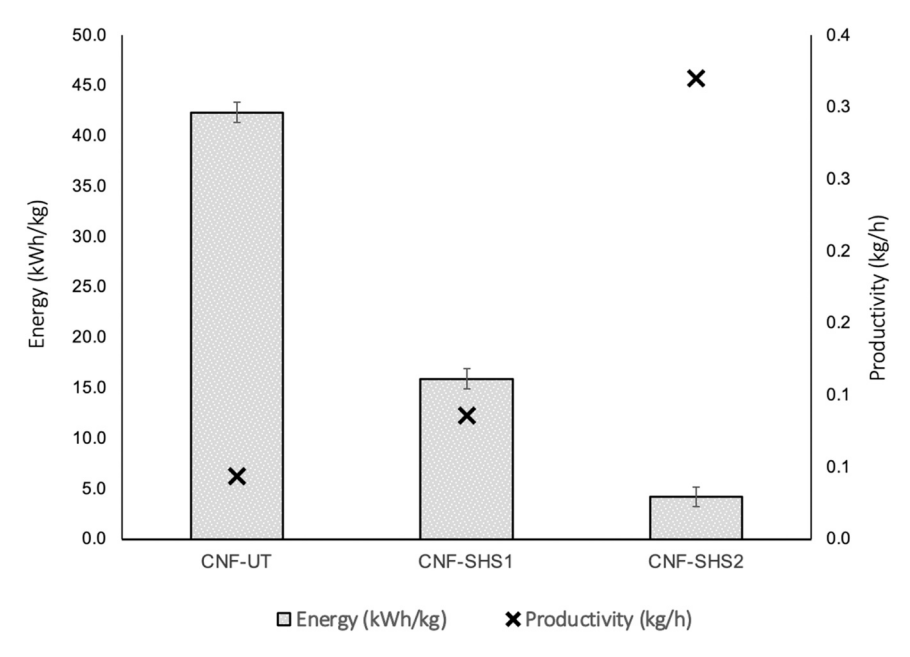


Fig. 8. Energy consumption (kWh/kg) and productivity (kg/h) of CNF production processed at 4 wt% solid content.

Table 4Data of viscosity and diameter size of 4 wt% CNF samples at actual cycles of wet disc mill.

Samples	UT	SHS1	SHS2
Viscosity at 25 °C (cP)	13200	8500	2580
Average diameter (nm)	33.90	28.65	25.08

^{*}Note: The data are presented with replicates

consumption during WDM processing by applying pretreatment of cellulose sample.

3.7. Economic assessment of the energy-neutral pretreatment for the production of cellulose nanofibrils from oil palm empty fruit bunch

The rising demand in the CNF market leads to an increased number of companies producing CNF processing. One of the major issues regarding its production, which is the energy consumption is being considered. Berglund et al. (2020) reported that by omitting the pretreatment, the energy demands and production cost of CNF can be reduced. In contrast, studies by Arvidsson et al. (2015) stated that energy-efficient production of CNFs can be achieved by the incorporation of pretreatment, which, however, leads to increased environmental

Table 5Comparison of energy consumption for CNF production.

Source of cellulose pulp	Pretreatment	Fibrillation process	Solid content (wt%)	Energy input (kWh/kg)	CNF diameter	Ref.
Spruce softwood	Thermostatic reactor	Microfluidizer	1 – 2	14.9	< 100 nm	Zimmermann et al. (2010)
Hardwood	Valley beater	Homogenizer	0.7	21.9	10 - 100 nm	Spence et al. (2011)
Hardwood	Valley beater	Wet-grinding	3	3.6	$\sim 20.5~\mu m$	
Triticale straw	TEMPO-mediated oxidation	Homogenizer	2	40.0 – 45.0	20 - 30 nm	Boufi and Gandini (2015)
Tunicate	Alkali/dimethyl sulfoxide swelling followed by esterification	Stirring	0.2	3.4	7.1 nm	Zhou et al. (2024)
Kraft eucalyptus	Valley beater	Wet-grinding	2	< 30.0	3 – 5 nm	Wang and Zhu (2016)
Kraft softwood	Endoglucanase enzyme	Wet-grinding	2	< 14.0	2-20 nm	Nair et al. (2014)
Kraft softwood	Endoglucanase enzyme	Wet-grinding	2	12.9	9 – 12 nm	Liu et al. (2018)
Bagasse	Endoglucanase enzyme	Wet-grinding	2	8.5	9 – 12 nm	
Oil palm empty fruit bunch	SHS treatment	Wet-grinding	1 – 4	4.2 – 7.4	6.7 – 50 nm	This work

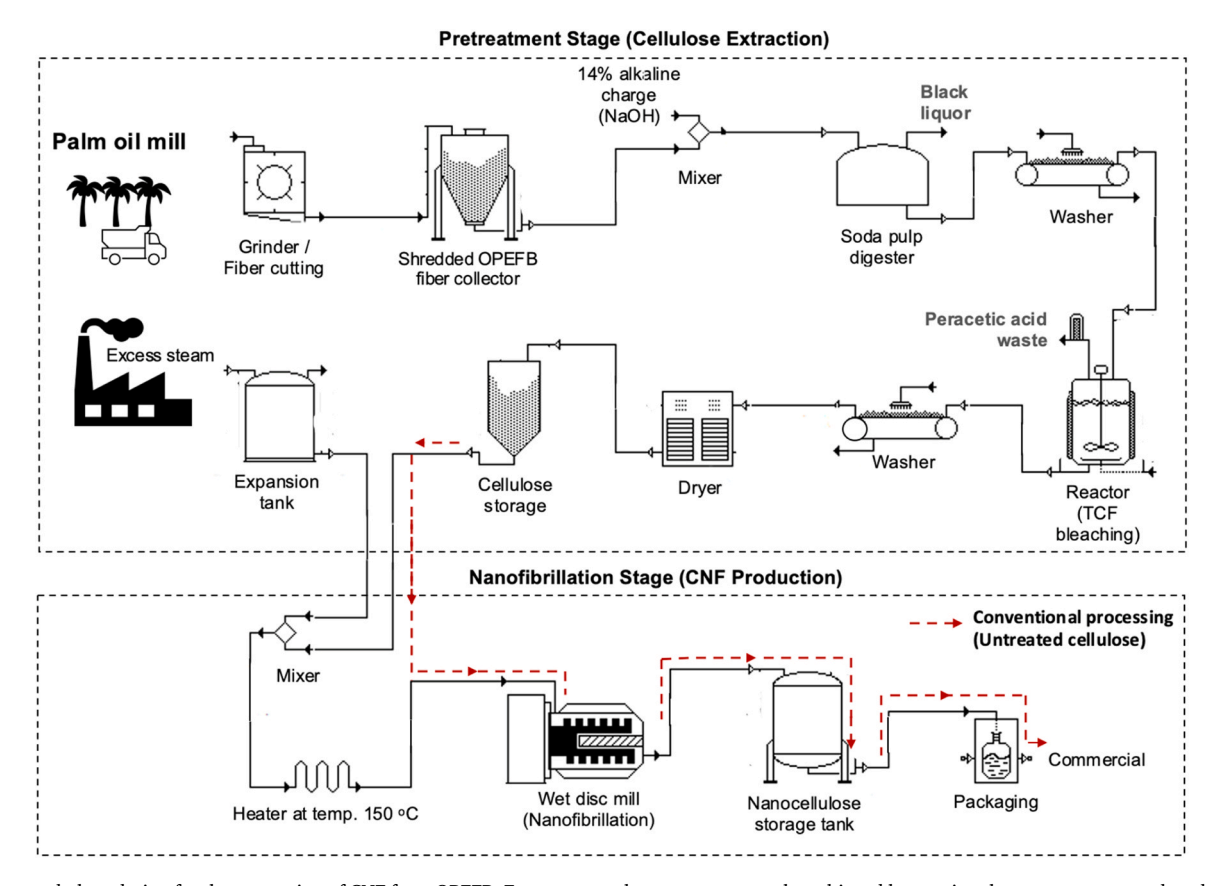


Fig. 9. Proposed plant design for the processing of CNF from OPEFB. Energy-neutral pretreatment can be achieved by tapping the excess steam produced at the palm oil mill. (Note: red dashed line indicates the flow for CNF-UT production with no SHS pretreatment).

impacts. In this work, the possibility of adopting pretreatment while reducing the environmental impact is demonstrated. This can be achieved by partnering with the palm oil mill to obtain the two important resources for the production of CNF, which are fiber (OPEFB) and steam (for the SHS pretreatment). Approximately, 177,000 tons of excess steam is produced annually from the palm oil mill due to the excessive burning of biomass as the source of energy (Abdullah et al., 2016; Chiew et al., 2011). This unused steam can be tapped and used as a source of energy for the CNF factory, and also for the SHS pretreatment in the processing line. This energy-neutral pretreatment can be realized if the CNF plant can be constructed next to the palm oil mill. The proposed plant design is shown in Fig. 9.

The cost structure of the proposed CNF processing plant is demonstrated in Table 6. The overall plant production costs were generated based on the target annual CNF production of approximately 1 ton. The calculation was made based on the technical data obtained from this study with the following details:

- i) Comparison was made between conventional processing and improved processing methods
- ii) Conventional processing involves the non-pretreated cellulose processing to produce CNF-UT, with solid content of 2 wt%
- iii) Improved processing refers to the use of SHS-pretreated cellulose to produce CNF-SHS2, with solid content of 4 wt%
- iv) Data used for CNF-UT: Productivity of 0.026 kg/h, Energy consumption of 50.5 kWh/kg
- v) Data used for CNF-SHS2: Productivity of 0.320 kg/h, Energy consumption of 4.2 kWh/kg,

The CAPEX and OPEX were calculated to evaluate the cost between CNF-UT and CNF-SHS2 production line in the CNF processing plant.

Table 6The economic assessment for the production of 1 ton CNF from plant processing

Items	CNF-UT, USD	CNF-SHS2, USD
CAPEX		
Purchase equipment cost	194,396	196,783
Building	19,440	19,678
Electrical systems	19,440	19,678
Total Plant Direct Cost	233,276	236,140
Engineering	11,664	11,807
Construction	69,983	70,842
Total Plant Indirect Cost	81,646	82,649
Total Plant Cost	314,922	318,788
Contractor's fees	9448	9564
Contingency	15,746	15,939
Total capital investment	340,116	344,292
OPEX		
Basic labour costs	39,692	3225
Fringe benefits	15,877	1290
Supervision	7938	645
Administration	19,846	1613
Total labour costs	83,354	6773
Raw material	5816	5816
Utilities	15,756	4633
Operating supply	3969	323
Laboratory/QC/QA	3969	323
Total variables costs	112,865	17,867
Depreciation	32,747	33,149
Maintenance and repair	6894	6979
Total fixed costs	39,641	40,128
Total production costs	152,506	57,995
Unit-production cost per kg	168	64
Profitability analysis		
Selling price per kg	240	240
Revenue per annum	217,680	217,680
Gross profit per annum	65,174	159,685
Net present value	91,827	714,031
Internal rate of return (%)	13 %	45 %
Project period (year)	10	10

Note: USD = United States Dollar

CAPEX is the total capital investment from the total cost of direct and indirect of the plants, as well as the fees of contractor and contingency. The direct cost of the plant includes the equipment purchase cost, building, yard improvement, and electrical system. The purchasing cost of major equipment was obtained according to the market price. Whereas, the indirect cost of the plant included the engineering and construction cost. The total capital investment (TCI) for the CNF-SHS2 production line was estimated at USD 344,292, which is higher compared to the CNF-UT. This is contributed by the high capital cost needed to spare steam from the palm oil mill to be utilized, thus, requiring additional costs for the unit operations such as heater, expansion tanks and mixer, and the cost for the construction.

OPEX on the other hand refers to the sum of total labour cost, total variables cost, and total fixed cost. Total labour cost includes basic labour costs, fringe benefits, supervision, and administration. The basic salary was calculated according to the Malaysia national minimum wage policy (Bank Negara Malaysia, 2020). The production plants were assumed to have management and production work up to 8 – 9 hours per day for 261 days in a year. The total variables cost (TVC) was calculated by including raw materials, utilities, consumables, operating supplies and laboratory QA/QC, whereby the CNF-SHS2 system has incurred a lower cost by 92 % compared to the CNF-UT system. Total fixed costs include depreciation of the equipment used and their maintenance expenditures, summing up the annual cost to bear at USD 40,128 per annum for the CNF-SHS2 system. By including all the expenditures, total production cost per annum for CNF-SHS2 is USD 57,995 with the projected unit-production cost per kg of CNF was USD 64. Compared to the CNF-UT system, it can be concluded that the CNF-SHS2 system outweighed the CNF-UT system by \sim 62 % in terms of economic feasibility.

The profitability analysis was calculated based on the selling price of CNF at USD 240, following the average market price for commercial CNF within the range of USD 100 – 500 (Future Markets Inc.., 2019). The annual gross profit for CNF-UT and CNF-SHS2 systems was projected at USD 65,174 and USD 159,685, respectively. The contribution to higher profit of CNF-SHS2 system was correlated to the higher production rate of 92.0 % than the CNF-UT system. Net present value (NPV) and internal rate of return (IRR) were determined to assess the profitability of an investment, where these values are critical for capital-budget decisions. Simply put, these values presume the value of the system as either worth investing in or not. The higher the values, the more desirable it becomes. By taking into account the current inflation rate of 6.6 % for 10 years, the NPV of the SHS-treated system was projected at USD 714,031, while the IRR achieved 45 %, signifying the project would provide a better chance of strong growth.

4. Conclusions

High energy consumption and low productivity of conventional CNFs processing have contributed to the high price of nanocellulose and hence its slow application and utilization at the commercial scale. In this research, it was exhibited that the energy consumption in nanocellulose processing can be lowered, and at the same time, the productivity can be improved by manipulating the cellulose degree of polymerization. Superheated steam pretreatment contributed to the alteration of the cellulose DP, in which reduced cellulose DP was found to reduce the viscosity of the CNF suspension and eventually caused less burden to the CNF processing due to less fiber entanglement and better flow property. These contributed to the ability to have high throughput processing, with faster processing per cycle compared to the one without pretreatment. This in overall, improved the productivity, reduced the energy consumption and hence, lowering the production costs. With the production cost reduction, the actual selling price of CNF can be reduced, and this will promote the application of the nanocellulose at the commercialization scale. The example shown in this article on the coupling of a nanocellulose production line with the palm oil mill is meant to tap the excess energy from the mill. In countries without palm

oil mills, other industries that can be self-sustained in terms of energy generation may adopt this idea for reducing the production cost. Pulping industry for instance may generate its own energy by utilizing the black liquor generated during pulping and will be able to contribute to the energy-neutral pretreatment process. In this case, the partnership between pulp, paper and nanocellulose mills would be advantageous in terms of lowering the production cost. Lower cost of nanocellulose production is expected to promote the mass production of CNF worldwide, and hence the selling price can be reduced and this will benefit the downstream industries utilizing nanocellulose.

Consent for publication / competing interests

The authors declare that they have read and understood that they have no significant competing financial, professional and/or personal interests that might have influenced the presentation work described in this manuscript. Also, the content of this manuscript was original and has never been reported.

Ethics approval and consent to participate

Not applicable

Authors' contributions

All authors had a significant participation in the development of this work. LNM: Perform experimental work, data collection, analyzing the data, writing and drafted of the manuscript; HA: Supervision, conceptual, visualization, writing-review and editing, funding acquisition; MRZ, YA, MAH: Conceptualization, supervision; funding acquisition; TATY-A: review and draft editing.

Funding

The publishing of this study was supported by the research grants given from our research institute, Universiti Putra Malaysia through GP-IPS (project no.: GP-IPS/2017/9519300) and GP-Berimpak (project no.: GPB/2017/9523000)

CRediT authorship contribution statement

Hidayah Ariffin: Writing – review & editing, Validation, Supervision, Resources, Project administration, Funding acquisition, Conceptualization. Liana Noor Megashah: Writing – original draft, Methodology, Investigation, Formal analysis, Data curation. Tengku Arisyah Tengku Yasim-Anuar: Investigation, Formal analysis. Mohd Ali Hassan: Writing – review & editing, Supervision, Resources. Yoshito Ando: Writing – review & editing, Supervision, Resources. Mohd Rafein Zakaria: Writing – review & editing, Supervision.

Declaration of Competing Interest

The authors declare the following financial interests/personal relationships which may be considered as potential competing interests: Hidayah Ariffin reports financial support was provided by Putra Malaysia University. If there are other authors, they declare that they have no known competing financial interests or personal relationships that could have appeared to influence the work reported in this paper.

Acknowledgments

The authors would like to thank our institute, Universiti Putra Malaysia (UPM) for providing financial support through GP-IPS and GP-Berimpak grants. Acknowledge gives to Forest Research Institute Malaysia (FRIM) for permission to use the digester for the pulping process. Our gratitude also goes to the Universiti Putra Malaysia School

of Graduate Studies (SGS) and the Ministry of Higher Education Malaysia for their technical support towards this student's project. Also thank to Seri Ulu Langat Palm Oil Mill at Dengkil Selangor, Malaysia for kindly supplied oil palm empty fruit bunch (OPEFB) fibers as the main raw material in this study.

Data availability

No data was used for the research described in the article.

References

- Abdullah, S.S.S., Shirai, Y., Ali, A.A.M., Mustapha, M., Hassan, M.A., 2016. Case study: preliminary assessment of integrated palm biomass biorefinery for bioethanol production utilizing non-food sugars from oil palm frond petiole. Energy Convers. Manag. 108, 233–242.
- Abe, K., Iwamoto, S., Yano, H., 2007. Obtaining cellulose nanofibers with a uniform width of 15 nm from wood. Biomacromolecules 8, 3276–3278.
- Alemdar, A., Sain, M., 2008. Isolation and characterization of nanofibers from agricultural residues: wheat straw and soy hulls. Bioresour. Technol. 99, 1664–1671.
- Alim, M.A., Moniruzzaman, M., Hossain, M.M., Wahiduzzaman, Repon, M.R., Hossain, I., Jalil, M.A., 2022. Manufacturing and compatibilization of binary blends of superheated steam treated jute and poly (lactic acid) biocomposites by meltblending technique. Heliyon 8, e09923. https://doi.org/10.1016/j.heliyon.2022. e09923.
- Ariffin, H., Norrrahim, M.N.F., Yasim-Anuar, T.A.T., Nishida, H., Hassan, M.A., Ibrahim, N.A., Yunus, W.M.Z.W., 2018. Oil Palm Biomass Cellulose-Fabricated Polylactic Acid Composites for Packaging Applications, in: Jawaid, M., Swain, S.K. (Eds.), Bionanocomposites for Packaging Applications. Springer, Cham, Cham.
- Arvidsson, R., Nguyen, D., Svanström, M., 2015. Life cycle assessment of cellulose nanofibrils production by mechanical treatment and two different pretreatment processes. Environ. Sci. Technol. 49, 6881–6890.
- Balea, A., Fuente, E., Tarrés, Q., Pèlach, M.À., Mutjé, P., Delgado-Aguilar, M., Blanco, A., Negro, C., 2021. Influence of pretreatment and mechanical nanofibrillation energy on properties of nanofibers from Aspen cellulose. Cellulose 28, 9187–9206.
- Bank Negara Malaysia, 2020. Labor market: Wages/Earnings | Bank Negara Malaysia | Central Bank of Malaysia [WWW Document]. URL \https://www.bnm.gov.my/index.php\ (accessed 2.14.20).
- Barchyn, D., Cenkowski, S., 2014. Process analysis of superheated steam pre-treatment of wheat straw and its relative effect on ethanol selling price. Biofuel Res. J. 1, 123–128. https://doi.org/10.18331/BRJ2015.1.4.4.
- Bardet, R., Bras, J., 2014. Cellulose nanofibers and their use in paper industry. Handb. Green, Mater. 207–232.
- Berglund, L., Breedveld, L., Oksman, K., 2020. Toward eco-efficient production of natural nanofibers from industrial residue: Eco-design and quality assessment. J. Clean. Prod. 255, 120274.
- Berglund, L., Noël, M., Aitomäki, Y., Öman, T., Oksman, K., 2016. Production potential of cellulose nanofibers from industrial residues: Efficiency and nanofiber characteristics. Ind. Crop. Prod. 92, 84–92.
- Boufi, S., Gandini, A., 2015. Triticale crop residue: a cheap material for high performance nanofibrillated cellulose. RSC Adv. 5, 3141–3151.
- Challabi, A.J.H., Chieng, B.W., Ibrahim, N.A., Ariffin, H., Zainuddin, N., 2019. Effect of superheated steam treatment on the mechanical properties and dimensional stability of PALF/PLA biocomposite. Polym. (Basel) 11.
- Chang, F., Lee, S.H., Toba, K., Nagatani, A., Endo, T., 2012. Bamboo nanofiber preparation by HCW and grinding treatment and its application for nanocomposite. Wood Sci. Technol. 46, 393–403.
- Chiew, Y.L., Iwata, T., Shimada, S., 2011. System analysis for effective use of palm oil waste as energy resources. Biomass-.-. Bioenergy 35, 2925–2935.
- Eriksen, Ø., Syverud, K., Gregersen, Ø., 2008. The use of microfibrillated cellulose produced from kraft pulp as strength enhancer in TMP paper. Nord. Pulp Pap. Res. J. 23, 299–304.
- Foster, E.J., Moon, R.J., Agarwal, U.P., Bortner, M.J., Bras, J., Camarero-Espinosa, S., Chan, K.J., Clift, M.J.D., Cranston, E.D., Eichhorn, S.J., Fox, D.M., Hamad, W.Y., Heux, L., Jean, B., Korey, M., Nieh, W., Ong, K.J., Reid, M.S., Renneckar, S., Roberts, R., Shatkin, J.A., Simonsen, J., Stinson-Bagby, K., Wanasekara, N., Youngblood, J., 2018. Current characterization methods for cellulose nanomaterials. Chem. Soc. Rev. 47, 2609–2679.
- $Future\ Markets\ Inc,\ 2019.\ Nanocellulose\ Investment\ and\ Pricing\ Guide\ 2019.$
- Ganesh Kumar, C., Pradeep Kumar, M., Gupta, S., Shyam Sunder, M., Veera Mohana Rao, K., Jagadeesh, B., Swapna, V., Kamal, A., 2015. Isolation and characterization of cellulose from sweet sorghum bagasse. Sugar Tech. 17, 395–403.
- Henriksson, M., Berglund, L., 2007. Structure and properties of cellulose nanocomposite films containing melamine formaldehyde. J. Appl. Polym. Sci. 106, 2817–2824.
- Henriksson, M., Berglund, L.A., Isaksson, P., Lindstro, T., 2008. Cellulose Nanopaper Structures of High Toughness 1579–1585.
- Hietala, M., Varrio, K., Berglund, L., Soini, J., Oksman, K., 2018. Potential of municipal solid waste paper as raw material for production of cellulose nanofibres. Waste Manag 80, 319–326.
- Huang, S., Wang, D., 2017. A simple nanocellulose coating for self-cleaning upon water action: molecular design of stable surface hydrophilicity. Angew. Chem. Int. Ed. 56, 9053–9057

- Hubbell, C.A., Ragauskas, A.J., 2010. Effect of acid-chlorite delignification on cellulose degree of polymerization. Bioresour. Technol. 101, 7410–7415.
- Hwangbo, S., Heo, J., Lin, X., Choi, M., Hong, J., 2016. Transparent superwetting nanofilms with enhanced durability at model physiological condition. Sci. Rep. 6.
- Ilyas, R.A., Sapuan, S.M., Ishak, M.R., 2018. Isolation and characterization of nanocrystalline cellulose from sugar palm fibres (Arenga pinnata). Carbohydr. Polym. 181, 1038–1051.
- Iwamoto, S., Abe, K., Yano, H., 2008. The effect of hemicelluloses on wood pulp nanofibrillation and nanofiber network characteristics. Biomacromolecules 9, 1022–1026.
- Iwamoto, S., Endo, T., 2015. 3 Nm thick lignocellulose nano fibers obtained from esterified wood with maleic anhydride. ACS Macro Lett. 4, 80–83.
- Josset, S., Orsolini, P., Siqueira, G., Tejado, A., Tingaut, P., Zimmermann, T., 2014.
 Energy consumption of the nanofibrillation of bleached pulp, wheat straw and recycled newspaper through a grinding process 3D Printing of Cellulose Reinforced Composites View project Porous Nanofibrillated Cellulose Functional Materials View project. Artic. Nord. Pulp Pap. Res. J. 29, 167–175.
- Julie Chandra, C.S., George, N., Narayanankutty, S.K., 2016. Isolation and characterization of cellulose nanofibrils from arecanut husk fibre. Carbohydr. Polym. 142, 158–166.
- Khazraji, A.C., Robert, S., 2013. Self-assembly and intermolecular forces when cellulose and water interact using molecular modeling. J. Nanomater. 2013, 12.
- Klemm, D., Kramer, F., Moritz, S., Lindström, T., Ankerfors, M., Gray, D., Dorris, A., 2011. Nanocelluloses: a new family of nature-based materials. Angew. Chem. Int. Ed. 50 (24), 5438–5466.
- Koistinen, A., Phiri, J., Kesari, K.K., Vuorinen, T., Maloney, T., 2023. Effect of pulp prehydrolysis conditions on dissolution and regenerated cellulose pore structure. Cellulose 30, 2827–2840. https://doi.org/10.1007/s10570-023-05050-w.
- Levanič, J., Šenk, V.P., Nadrah, P., Poljanšek, I., Oven, P., Haapala, A., 2020. Analyzing TEMPO-oxidized cellulose fiber morphology: new insights into optimization of the oxidation process and nanocellulose dispersion quality. ACS Sustain. Chem. Eng. 8, 17752-17762
- Ling, Z., Wang, T., Makarem, M., Santiago Cintrón, M., Cheng, H.N., Kang, X., Bacher, M., Potthast, A., Rosenau, T., King, H., Delhom, C.D., Nam, S., Vincent Edwards, J., Kim, S.H., Xu, F., French, A.D., 2019. Effects of ball milling on the structure of cotton cellulose. Cellulose 26, 305–328.
- Liu, X., Jiang, Y., Qin, C., Yang, S., Song, X., Wang, S., Li, K., 2018. Enzyme-assisted mechanical grinding for cellulose nanofibers from bagasse: energy consumption and nanofiber characteristics. Cellulose 25, 7065–7078.
- Malucelli, L.C., Matos, M., Jordão, C., Lomonaco, D., Lacerda, L.G., Carvalho Filho, M.A. S., Magalhães, W.L.E., 2019. Influence of cellulose chemical pretreatment on energy consumption and viscosity of produced cellulose nanofibers (CNF) and mechanical properties of nanopaper. Cellulose 26, 1667–1681.
- Marx-Figini, M., 1978. Significance of the intrinsic viscosity ratio of unsubstituted and nitrated cellulose in different solvents. Die Angew. Makromol. Chem. 72, 161–171.
- Megashah, L.N., Ariffin, H., Zakaria, M.R., Hassan, M.A., 2018a. Properties of cellulose extract from different types of oil palm biomass. IOP Conf. Ser. Mater. Sci. Eng. 368, 012049
- Megashah, L.N., Ariffin, H., Zakaria, M.R., Hassan, M.A., 2018b. Multi-step pretreatment as an eco-efficient pretreatment method for the production of cellulose nanofiber from oil palm empty fruit bunch. Asia-Pac. J. Mol. Biol. Biotechnol. 26, 1–8.
- Megashah, L.N., Ariffin, H., Zakaria, M.R., Hassan, M.A., Andou, Y., Padzil, F.N.M., 2020. Modification of cellulose degree of polymerization by superheated steam treatment for versatile properties of cellulose nanofibril film. Cellulose 27, 7417–7429.
- Morais, J.P.S., Rosa, M.D.F., De Souza Filho, M.D.S.M., Nascimento, L.D., Do Nascimento, D.M., Cassales, A.R., 2013. Extraction and characterization of nanocellulose structures from raw cotton linter. Carbohydr. Polym. 91, 229–235.
- Nair, S.S., Zhu, J.Y., Deng, Y., Ragauskas, A.J., 2014. Characterization of cellulose nanofibrillation by micro grinding. J. Nanopart. Res. 16, 2349.
- Peters, M.S., Timmerhaus, K.D., West, R.E., 2003. Plant design and economics for chemical engineers. McGraw-Hill chemical engineering series. McGraw-Hill Education.
- Qin, Y., Qiu, X., Zhu, J.Y., 2016. Understanding longitudinal wood fiber ultra-structure for producing cellulose nanofibrils using disk milling with diluted acid prehydrolysis. Sci. Rep. 6.
- Rajaratanam, D.D., Ariffin, H., Hassan, M.A., Kawasaki, Y., Nishida, H., 2017. Effects of (R)-3-hydroxyhexanoate units on thermal hydrolysis of poly((R)-3-hydroxybutyrate-

- co-(R)-3-hydroxyhexanoate)s. Polym. Degrad. Stab. 137, 58–66. https://doi.org/10.1016/j.polymdegradstab.2017.01.007.
- Rambabu, N., Panthapulakkal, S., Sain, M., Dalai, A.K., 2016. Production of nanocellulose fibers from pinecone biomass: evaluation and optimization of chemical and mechanical treatment conditions on mechanical properties of nanocellulose films. Ind. Crops Prod. 83, 746–754.
- Ramírez, C.A.R., Rol, F., Bras, J., Dufresne, A., Garcia, N.L., Accorso, N.D., 2019. Isolation and characterization of cellulose nanofibers from argentine tacuara cane (Guadua angustifolia Kunth. J. Renew. Mater. 7, 373–381.
- Rojas, J., Bedoya, M., Ciro, Y., 2015. Current Trends in the Production of Cellulose Nanoparticles and Nanocomposites for Biomedical Applications, in: Cellulose -Fundamental Aspects and Current Trends. InTech.
- Rol, F., Karakashov, B., Nechyporchuk, O., Terrien, M., Meyer, V., Dufresne, A., Belgacem, M.N., Bras, J., 2017. Pilot-scale twin screw extrusion and chemical pretreatment as an energy-efficient method for the production of nanofibrillated cellulose at high solid content. ACS Sustain. Chem. Eng. 5, 6524–6531.
- Sánchez, R., Espinosa, E., Domínguez-Robles, J., Loaiza, J.M., Rodríguez, A., 2016. Isolation and characterization of lignocellulose nanofibers from different wheat straw pulps. Int. J. Biol. Macromol. 92, 1025–1033.
- Segal, L., Creely, J.J., Martin, A.E., Conrad, C.M., 1959. An empirical method for estimating the degree of crystallinity of native cellulose using the x-ray diffractometer. Text. Res. J. 29, 786–794.
- Shahabi-Ghahfarrokhi, I., Khodaiyan, F., Mousavi, M., Yousefi, H., 2015. Preparation and characterization of nanocellulose from beer industrial residues using acid hydrolysis/ultrasound. Fibers Polym. 16, 529–536.
- Siró, I., Plackett, D., 2010. Microfibrillated cellulose and new nanocomposite materials: a review. Cellulose 17, 459–494.
- Spence, K.L., Venditti, R.A., Rojas, O.J., Habibi, Y., Pawlak, J.J., 2011. A comparative study of energy consumption and physical properties of microfibrillated cellulose produced by different processing methods. Cellulose 18, 1097–1111.
- Tayeb, A.H., Amini, E., Ghasemi, S., Tajvidi, M., 2018. Cellulose nanomaterials-binding properties and applications: a review. Molecules 23, 1–24.
- Teixeira, R.S.S., Silva, A.S. da, Bon, E.P.S., Kim, H.-W., Jang, J.-H., Ishikawa, K., Lee, S.-H., Endo, T., 2015. Combining biomass wet disk milling and endoglucanase/ \hat{I}^2 -glucosidase hydrolysis for the production of cellulose nanocrystals. Carbohydr. Polym.
- Thi, T., Ho, T., Abe, K., 2015. Nanofibrillation of pulp fibers by twin-screw extrusion. Cellulose 22, 421–433.
- Wang, W., Mozuch, M.D., Sabo, R.C., Kersten, P., 2015a. Production of cellulose nanofibrils from bleached eucalyptus fibers by hyperthermostable endoglucanase treatment and subsequent microfluidization. Cellulose 351–361.
- Wang, W., Sabo, R.C., Mozuch, M.D., Kersten, P., Jin, J.Y.Z.Y., 2015b. Physical and mechanical properties of cellulose nanofibril films from bleached eucalyptus pulp by endoglucanase treatment and microfluidization. J. Polym. Environ.
- Wang, Q., Zhu, J.Y., 2016. Effects of mechanical fibrillation time by disk grinding on the properties of cellulose nanofibrils. Tappi J. 15, 419–423.
- Yang, W., Jiao, L., Min, D., Liu, Z., Dai, H., 2017. Effects of preparation approaches on optical properties of self-assembled cellulose nanopapers. RSC Adv. 7, 10463–10468.
- Yasim-Anuar, T.A.T., Ariffin, H., Hassan, M., 2018. Characterization of cellulose nanofiber from oil palm mesocarp fiber produced by ultrasonication. IOP Conf. Ser. Mater. Sci. Eng. 368, 1–11.
- Yasim-Anuar, T.A.T., Sharip, N.S., Megashah, L.N., Ariffin, H., Nor, N.A.M., 2020. Cellulose nanofibers from waste paper and their utilization as reinforcement materials in poly((r)-3-hydroxybutyrate-co-(r)-3-hydroxyhexanoate bionanocomposite. Pertanika J. Sci. Technol. 28, 259–271.
- Zhao, Y., Xu, C., Xing, C., Shi, X., Matuana, L.M., Zhou, H., Ma, X., 2015. Fabrication and characteristics of cellulose nanofibril films from coconut palm petiole prepared by different mechanical processing. Ind. Crops Prod. 65, 96–101.
- Zhou, M., Chen, D., Chen, Q., Chen, P., Song, G., CHang, C., 2024. Reversible surface engineering of cellulose elementary fibrils: from ultralong nanocelluloses to advanced cellulosic materials. Adv. Mater. 36, 2312220.
- Zhu, J.Y., Sabo, R., Luo, X., 2011. Integrated production of nano-fibrillated cellulose and cellulosic biofuel (ethanol) by enzymatic fractionation of wood fibers. Green. Chem. 13, 1339–1344.
- Zimmermann, T., Bordeanu, N., Strub, E., 2010. Properties of nanofibrillated cellulose from different raw materials and its reinforcement potential. Carbohydr. Polym. 79, 1086–1093.